

EXPERIMENTAL STUDY ON FLEXURAL BEHAVIORS OF ENGINEERED CEMENTITIOUS COMPOSITE BEAMS REINFORCED WITH FRP BARS

F. YUAN^{*}, J.L. PAN[†]

^{*} Key Laboratory of Concrete and Prestressed Concrete Structures of Ministry of Education
School of Civil Engineering, Southeast University, Nanjing, China
e-mail: yf_1542@163.com

[†] Key Laboratory of Concrete and Prestressed Concrete Structures of Ministry of Education
School of Civil Engineering, Southeast University, Nanjing, China
e-mail: jinlongp@gmail.com

Key words: FRP, ECC, Flexural behavior, Crack width, Ductility, Durability

Abstract: The use of FRP reinforcement has attracted great attention in concrete structures due to its high tensile strength, good fatigue performance, and especially inherent anti-corrosion ability. Engineered cementitious composite (ECC) is a class of high performance cementitious composites with pseudo strain-hardening and multiple cracking properties. Substitution of concrete with ECC can avoid the cracking and durability problems from weakness of concrete. In this paper, a kind of FRP reinforced ECC beam is proposed to obtain super high durability and better mechanical performance compared with normal steel reinforced concrete beam. Six FRP reinforced ECC or ECC/concrete composite beams with various longitudinal and transverse reinforcement ratios and ECC thicknesses have been tested. According to the test results, FRP reinforced ECC beams show better flexural properties in terms of load carrying capacity, shear resistance, ductility, and damage tolerance compared with FRP reinforced concrete beams. For the FRP reinforced ECC beam without stirrups, although it finally fails in shear mode, its flexural load capacity and ultimate deformation are comparable to the FRP reinforced concrete beams with proper designed stirrups, and the failure process is ductile due to strain hardening behavior of ECC materials. For ECC/concrete composite beams, partially application of ECC can lead to considerable increase of load capacity, energy dissipation. When the ECC layer is placed in the tension zone, the crack width along the beam can be well controlled, and hence high residual strength and stiffness of the composite beam can be expected.

1 INTRODUCTION

FRP reinforcement is highly suitable for concrete structures subjected to corrosive environments, such as concrete pavements treated with de-icing salts, waste water and chemical treatment plants, and structures built in or close to sea water. Furthermore, the lightweight nature of FRPs is a distinct advantage for weight sensitive structures. The nonmagnetic characteristic makes FRP feasible for reinforcing facilities and structures

supporting magnetic resonance imaging units or other equipment sensitive to electromagnetic fields. However, the widely used of FRP reinforcement is limited due to two major inherent drawbacks of FRP materials: low modulus of elasticity and lack of ductility [1-2].

Generally speaking, the modulus of elasticity of most FRP materials is lower than that of steel, which causes larger deflection and crack width compared with conventional

RC members for a given reinforcement ratio. Serviceability criteria will control the design of FRP-reinforced members. Crack width has to be limited with respect to aesthetic consideration and special requirement of water-retaining structures, even though corrosion is not an issue for FRP-reinforced members.

Typically, steel reinforced concrete sections are designed in tension-controlled failed mode, which exhibits concrete crushing after sufficient steel yielding deformation. Sufficient yielding behaviour of steel reinforcement is referred to as ductile behaviour, which consumes substantial inelastic energy and provides a warning of impending failure. FRP bars often fail by brittle rupture under uniaxial tension and the failure is regarded as catastrophic. For FRP-reinforced concrete members, over-reinforced concept is adopted to avoid the brittle rupture of FRP reinforcement [3-4]. For over-reinforced concrete beams, a gradual failure can be obtained due to nonlinear compression failure of concrete in the compression zone. Investigation by Nanni [5] indicated that the balanced reinforcement ratio, which is defined as the reinforcement ratio producing a simultaneous failure of the concrete and the FRP reinforcement, was much lower than the practically adopted value. Two effective approaches for developing the strain capacity of FRP reinforcement had been put forward, which were expected to improve the ductility of FRP-reinforced beams. One is through the use of ductile hybrid FRP reinforcement. Harris et al [6] tested the hybrid FRP-reinforced concrete beams and found that the ductility of these beams was close to the conventional RC beam. The other is through the use of materials that have higher compressive strain capacity in the compression zone of the member. Naaman [7] proposed to use slurry infiltrated fibre concrete (SIFCON) to improve the ductility of FRP reinforced beams and Zhou [8] put forward to setting up compression yielding (CY) block in the compression zone of the beam. A large amount of ductility was acquired by developing a plastic hinge zone in the compression zone.

In recent years, a class of high performance fiber reinforced cementitious composites (called engineered cementitious composites) with ultra-ductility, has been developed for applications in construction industry [9-11]. ECC and concrete have similar ranges of tensile (4-6 MPa) and compressive strengths (30-80 MPa), while they behave distinct difference in tensile deformation. For conventional concrete, it fails in a brittle manner once its tensile strength is reached. However, for an ECC plate under uniaxial tension, after first cracking, tensile load capacity continues to increase with strain hardening behaviour accompanied by multiple cracks along the plate. For each individual crack, the crack tends to open steadily up to a certain crack width, and increasing loading will result in formation of an additional crack. With the same cracking mechanism, cracking of the ECC member can reach a saturated state with small crack spacing, which is determined by the stress transfer capacity of the fibres in the matrix. With increasing loading, a random single crack localizes and softening behaviour is followed. Typically, mechanical softening starts at a tensile strain of 3%-5%, with a crack spacing of 3-6 mm and crack width of about 60 μm [12]. In compression, ECC has a similar strength as concrete while the strain at the ultimate strength is nearly two times that of concrete. Previous studies have indicated that the compatible deformation between ECC and steel reinforcement can lead to decreased interfacial bond stresses and elimination of bond splitting cracks and surface spalling [13]. Flexural members exhibit significant increases in terms of ductility, load carrying capacity, shear resistance and damage tolerance if concrete is replaced by ECC material [14]. These unique properties make ECC material desirable for work in conjunction with FRP reinforcement to improve ductility and durability for FRP reinforced flexural members.

In this paper, several FRP reinforced ECC or ECC/concrete composite beams have been tested to verify the contribution of ECC material on ductility of flexural members. The influence of different parameters, including

longitudinal reinforcement ratio, ECC thickness, usage of shear reinforcement or not, on the ultimate strength, deformation capacity, and ductility, etc., are evaluated.

2 EXPERIMENTAL PROGRAM

2.1 Material properties

With the consideration of environmental sustainability, high volume of fly ash was used for making ECC materials in this experiment. The volume ratio of fly ash reached 80% of all cementitious material. In order to evaluate the ductility behavior of ECC used for FRP reinforced ECC or ECC/concrete composite beams, direct tensile tests were conducted on the specimens with dimension of 350 mm×50 mm×15 mm. Fig. 1 shows the tensile stress-strain curves of ECC materials. The test results indicated that the tensile strength exceeded 5MPa and the ultimate tensile strain approached 4%. Meanwhile, a number of cylinder specimens with dimension of 75 mm in diameter and 150 mm in height were tested in compression to obtain the compressive strength of ECC and concrete. The compressive strength of ECC and concrete are 38.3 MPa and 47.2 MPa respectively, and the elastic modulus of ECC and concrete are 15.50 GPa and 34.49 GPa respectively. Two types of BFRP bars with the diameter of 12 mm and 20 mm were used as the tensile reinforcement for the FRP reinforced beams. The surface of FRP bars is spirally wrapped with basalt fiber braid and sand particles are attached on the surface to enhance the bonding strength between FRP bars and concrete or ECC. Table 1 shows the

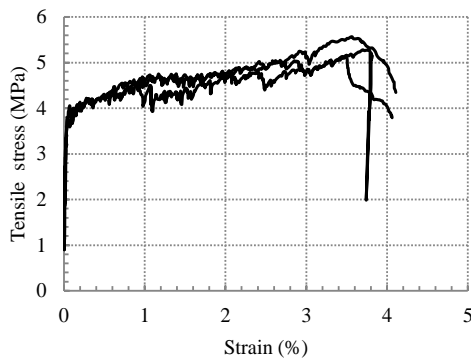


Figure 1: Tensile stress-strain relationship of ECC.

mechanical properties of BFRP reinforcement. The FRP bars exhibits linear elastic behaviour up to brittle failure. The elastic modulus and yield strength of steel bar are 200 GPa and 460 MPa, respectively.

2.2 Specimen preparation

Totally six beam specimens were tested to investigate the flexural behaviors of FRP reinforced ECC or ECC/concrete composite beams. Table 2 shows the details of each specimen. Since BFRP bars are used as the reinforcement, all beams are designed based on over-reinforced concept for avoiding brittle fracture of FRP reinforcement and increasing ductility of the beams. Hence, the reinforcement ratio of each beam specimen is larger than the balanced reinforcement ratio ρ_b . The beam specimens in the experimental program can be divided into two series. Series I consists of four FRP reinforced ECC beams with different longitudinal and transverse reinforcement ratios. Series II includes two FRP reinforced ECC/concrete composite beams with different ECC arrangements. The notation of the beam specimens is as follows. For each beam specimen, the first two characters of the notation 'BR' mean the beam is longitudinally reinforced with BFRP bars. The third character, 'E' or 'C', represents the matrix type of ECC or concrete respectively. The number '12' or '20', indicates the diameter of the longitudinal BFRP bar and characters 'ns' represent the beam specimen without stirrups. Therefore, 'BRE12' represents a BFRP reinforced ECC beam with bar diameter of 12 mm. 'BREC-C' stands for a BFRP reinforced ECC/concrete composite beam with a 90mm ECC layer from the top surface in the compression zone, and 'BREC-T' means a BFRP reinforced ECC/concrete

Table 1: Material properties of steel and FRP bars

Diameter (mm)	Tensile Modulus of elasticity E_f (GPa)	Ultimate tensile strength f_u (MPa)	Ultimate strain in tension, ε_{fu} , %
12	45	1088	2.4
20	46.2	907	1.96

Table 2: Summary of specimen information

Series	Specimen ID	Longitudinal reinforcement ratio (%)	Shear reinforcement (mm)	Matrix type
I	BRE12	0.377	$\phi 8@100$	ECC
	BRE20	1.05	$\phi 8@100$	ECC
	BRC20	1.05	$\phi 8@100$	Concrete
	BRE20-ns	1.05	---	ECC
II (composite)	BREC-C	1.05	$\phi 8@100$	90 mm ECC layer in compression zone
	BREC-T	1.05	$\phi 8@100$	90 mm ECC layer in tension zone

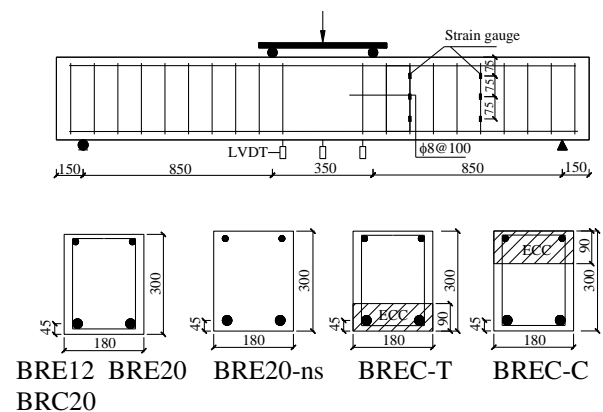
composite beam with a ECC layer of 90 mm from the bottom surface in the tension zone. The ECC layer of 90 mm is selected to ensure the ECC layer had the same centroid as the BFRP reinforcement, which was proved to be an effective way to increase the bond between ECC and BFRP reinforcement [15]. For casting of the ECC/concrete composite specimens, the ECC material was firstly cast. The plain concrete was prepared and cast on top of ECC layer after ECC layer was reached initial set for preventing the penetration of fresh concrete into ECC layer [15]. For ECC/concrete composite beam, transverse grooves on the ECC layer at every 100 mm were made to improve bond strength between concrete and ECC layer. The surface treatment is shown in Fig. 2. For all specimens except for BRE20-ns, the steel bars with diameter of 8 mm were used as shear reinforcement. For each beam specimens, the steel reinforcement of 8 mm was also used as the compression

**Fig 2 :** Schematic of surface treatment

steel reinforcement and supports for the stirrups along the beam. The main reason for not casting the plain concrete immediately after casting the ECC material was to prevent the penetration of fresh concrete into ECC layer [15]. For ECC/concrete composite beam, transverse grooves on the ECC layer at every 100 mm were made to prevent delamination between concrete and ECC layer. The surface treatment is shown in Fig. 2. For all specimens except for BRE20-ns, the steel bars with the diameter of 8 mm were used as shear reinforcement. For each beam specimens, the steel reinforcement of 8 mm was also used as the compression steel reinforcement and supports for the stirrups along the span.

2.3 Test setup

Each beam was loaded under four-point bending with loading span of 350 mm. The loading configuration is shown in Fig. 3. Three linear variable differential transformers

**Fig 3:** Schematic of test setup and specimen details

(LVDTs) were instrumented to monitor the mid-span deflection as well as the curvature of the beam. The strain variations of two steel stirrups were measured to determine whether the steel stirrups were yielded during the loading process. For the two stirrups, one is 375 mm from the middle span, and the other is 675 mm from the middle span. The distribution of strain gauges along the stirrup is shown in Fig. 3. The load was incrementally applied by a hydraulic jack and measured with a load cell. All the beams were loaded up to failure (corresponding to 80% of its peak load), followed by an unloading process for the purpose of achieving the elastic energy.

3 EXPERIMENTAL RESULTS AND DISCUSSIONS

3.1 Load-deflection responses and failure modes

Series I

The load-deflection curves for specimens of series I are shown in Fig. 4. For specimen BRE12, which is a FRP reinforced ECC beam with a longitudinal reinforcement ratio of 0.419%, initial tiny cracks occurred at a load of 29.7 kN in the pure bending region. After that, the slope of the curve showed a slight drop and kept almost constant until the peak load was reached, as shown in Fig. 4. With increasing bending moment, multiple inclined flexural shear cracks occurred outside the pure bending region and extended to a distance approximately 160 mm from the top surface of the beam. When the external load reached 165.6 kN, the outermost fiber of ECC in the compression zone reached the ultimate strain and started to crush. Almost at the same time, the BFRP reinforcement reached its tensile strength and fractured, followed by a sudden drop of external loading. Specimen BRE12 failed in a balanced failure mode, which indicated that strains in ECC and BFRP bars reached their ultimate values simultaneously. Based on a section analysis and an assumption of ECC ultimate strain capacity of 0.006, the balanced reinforcement ratio (ρ_b) of an ECC beam with the same details as beam BRE12 is

calculated to be 0.204%. However, beam BRE12 reached a balanced failure at a reinforcement ratio of 0.377%, which may be due to significant increase of ECC strain capacity under well confinement in the compression zone. The final crack pattern of BRE12 is shown in Fig. 5(a).

Specimen BRE20 has the same geometric dimensions and matrix type as specimen BRE12, but higher reinforcement ratio. The initial tiny crack occurred at the loading level of 39.2 kN in the pure bending region. The crack propagation was similar to specimen BRE12 before peak load, while the flexural stiffness is obviously larger than BRE12 due to higher longitudinal reinforcement ratio. The failure of the beam was initiated by crushing of ECC in the compression zone at a load of 238.6 kN with the mid-span deflection of 43.9 mm. Afterwards, the beam maintained substantial inelastic deformations without a significant loss of load carrying capacity, indicating that the specimen showed better ductility than BRE12. The maximum crack width of the beam was measured to be below 0.4mm until final failure. Specimen BRE20 finally failed by crushing of ECC in the compression zone with the displacement in the middle span of 75 mm and corresponding load of 185.1 kN. Compared with specimen BRE12, specimen BRE20 had larger compression zone due to much higher longitudinal reinforcement ratio, resulting in much higher load capacity. Furthermore, ECC showed much higher deformability under compression, which could work as a plastic hinge in the middle span and provide definite ductility for the BFRP reinforced ECC beam. Final crack pattern for beam BRE20 is shown in Fig. 5(b).

Specimen BRC20 has identical reinforcement details with BRE20, while the matrix is replaced by concrete. The load-deflection curves of two beams are coincident before initial flexural crack occurs, but the flexural stiffness of specimen BRE20 after first cracking is nearly 30% larger than that of specimen BRC20 due to cracking controlling ability of ECC materials. The load-carrying capacity and ultimate deflection of BRE20 are nearly 20% and 50% higher than those of

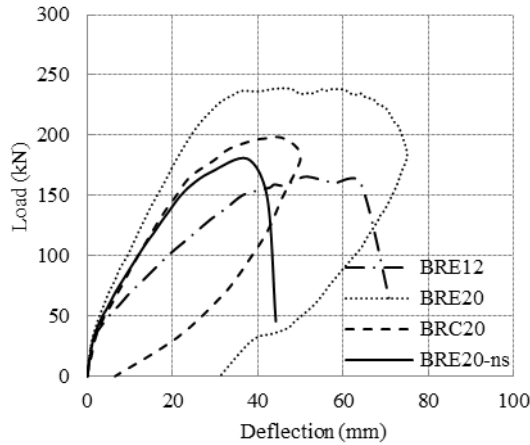


Fig 4: Load-deflection curves for series I

BRC20, respectively. For specimen BRC20, concrete crushing in the compression zone was observed at the load of 178.3 kN. However, this phenomenon was not observed for BRE20. In the ultimate stage, only about 10 evident flexural or shear cracks were observed along the beam span for specimen BRC20, while hundreds of tiny cracks were observed with a crack spacing of about 6-8 mm for specimen BRE20. It means that substitution of concrete with ECC for the BFRP reinforced beam can significantly decrease crack width and improve flexural stiffness of the beam, resulting in high post-peak strength and energy absorption of the beam, as well as high durability of the beam. Specimen BRC20 finally failed by concrete crushing in the compression zone with serious surface spalling, as shown in Fig. 5(c).

Specimen BRE20-ns has the same matrix type and geometric dimensions as BRE20, but without shear reinforcement along the span. The initial tiny crack occurred at a load level of 38.8 kN in the pure bending region. After initial crack occurred, the deformation in the middle of the span continued to increase with the external loading, accompanied by appearing of multiple cracks along the beams. With increasing external loading, more and more cracks occurred along the shear span until a saturated cracking state was reached at a load level of 180.5 kN with a corresponding deflection of 37.5 mm. With further increase of external loading, a random inclined shear crack localized, indicating peak strength of

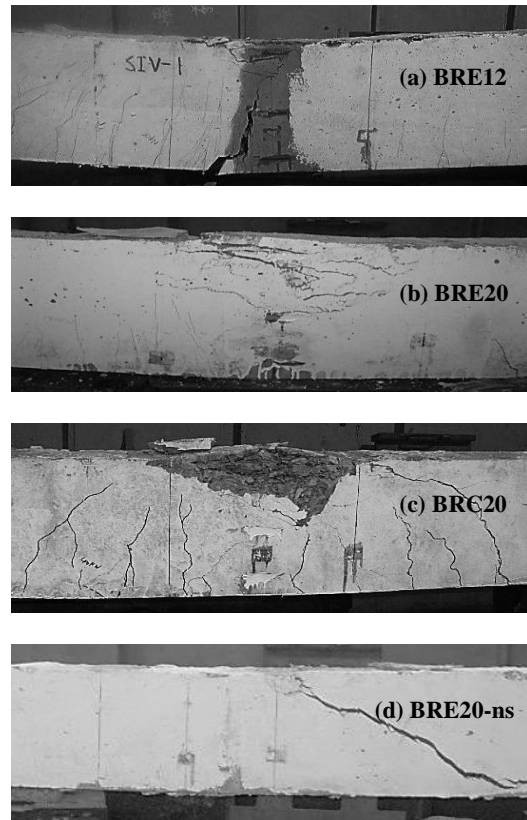


Fig 5 : Failure modes of beam series I

beam BRE20-ns was reached. With further increase of deformation, previous tiny cracks continued to propagate and open with sharp decrease of external load until final failure. The ultimate strength and corresponding deflection of BRE20-ns are just 8.9% and 17.4% lower than those of BRC20 respectively. According to the test results, the shear capacity of the ECC beam is 90.25 kN, which is nearly 1.73 times that of plain concrete beam (51.9 kN) with the same axial compressive strength of concrete and geometric dimensions. The shear capacity of plain concrete beam is calculated according to ACI Building code 318M-05. The final crack pattern of BRE20-ns is shown in Fig. 5(d).

Series II

The load-deflection curves for specimens of series II are shown in Fig. 6. Due to the higher cost of ECC materials compared with normal commercial concrete, application of ECC for a whole structure is essentially uneconomic. In this experiment, FRP reinforced ECC/concrete composite beams were designed in series II.

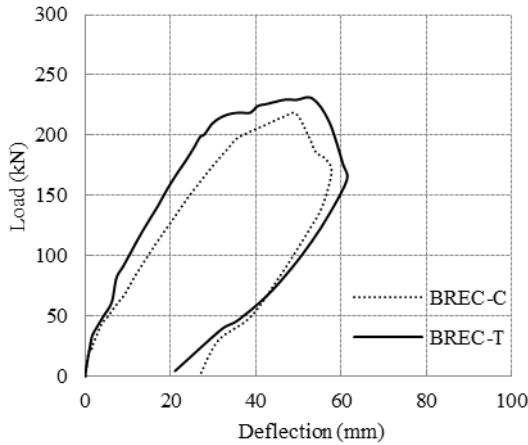


Fig 6 : Load-deflection curves for series II

For specimen BREC-C, an ECC layer of 90 mm was cast in the compression zone along the span. While for specimen BREC-T, the ECC layer with the same thickness was designed at the bottom of the tensile side.

For specimen BREC-C, initial flexural cracks occurred at the load level of 43 kN. With increasing external loading, more and more flexural shear cracks occurred along the shear span. When the load reached 217.6 kN, the beam failed by occurrence of a major shear crack under one of the loading points, accompanied by rupture of BFRP reinforcement in this cracked section. After that, the external load sharply decreased with further increase of deflection in the middle span until final failure. The ultimate failure pattern of beam BREC-C is shown in Fig. 7(a). Due to much higher compressive strain capacity of ECC compared with concrete, the compressive side of beam BREC-C remained intact even in the ultimate load stage. The load carrying capacity and ultimate deformation capacity of BREC-C are 9.2% and 12% larger than those of the concrete beam BRC20 respectively. The specimen BREC-C finally failed by BFRP rupture at the major shear crack section due to high sensitivity of BFRP reinforcement to transverse stress concentration, which significantly affected the ultimate load capacity and ductility of the beam.

For the ECC/concrete composite beam BREC-T, the first crack appeared in the middle span at a load level of 39.9 kN. With

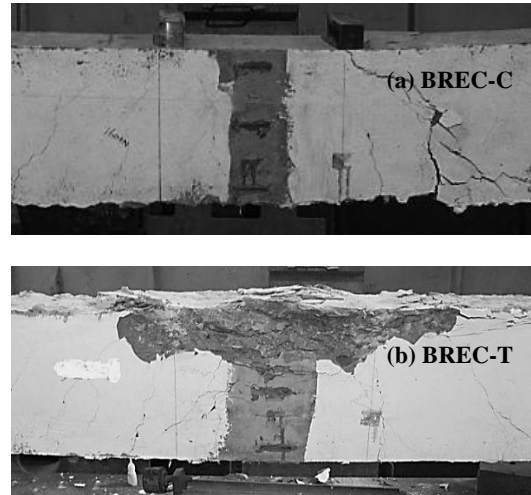


Fig 7 : Failure modes of beam series II



Fig 8 : Crack diffusion behavior in beam BREC-T

increasing external loading, many tiny cracks developed in ECC layer as well as in concrete within the tensile zone. It was interesting to find that wide cracks in concrete layer diffused into multiple fine cracks in the ECC layer, as shown in Fig. 8. Meanwhile, ECC has super high deformability and it can deform compatibly with FRP reinforcement so that bond splitting can be avoided during the loading process. The smeared crack distribution of BREC-T greatly reduced the tensile or shear stress concentration in the reinforcement at the cracked sections so that shear rupture of BFRP reinforcement can be avoided. No sign of delamination between the concrete and ECC layer was observed during the loading process, which proved that the surface treatment was effective for preventing delamination between ECC layer and concrete. The beam finally

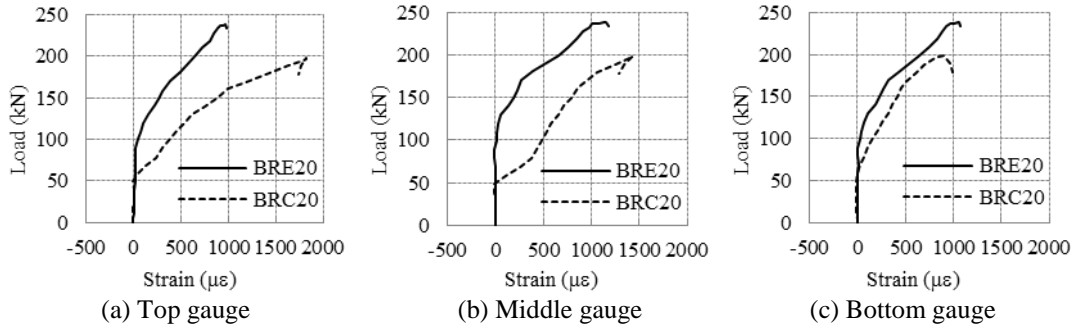


Fig 9 : Strains variations in stirrups for specimens BRE20 and BRC20

failed by concrete crushing in the compression zone. The final crack pattern of beam BREC-T is shown in Fig. 7(b). Compared with the concrete beam BRC20, BREC-T shows 16.8% and 28.6% higher peak load and corresponding deflection respectively, which is attributed to the fiber bridging effect of ECC in the tension zone.

3.2 Strain analysis

To avoid shear failure of a beam, a number of steel stirrups are used to increase the shear capacity of the beam. Under shear stresses, concrete material shows low strength and fails in a brittle mode. Although tensile or shear strength of ECC material is relative low (4-6 MPa), it shows superior ductile behavior in tension or shear. When ECC is applied for flexural members, its ductile behaviors in tension or shear can help to restrain opening of cracks and increase the load and deformation capacity. Fig. 9 shows the comparisons of average stirrup strains at different locations for BRE20 and BRC20. Since both of the beams failed in flexural mode, the strain values for all stirrups did not exceed the yielding strain before final failure. However, the developing process of strain values was distinctly different for the two beams. It can be found from Fig. 9 that the strain values of the concrete beam BRC20 fluctuated around 0 before the applied load reached around 50 kN (the first crack occurred in this section at this loading level). While for the ECC beam BRE20, the strain values fluctuated around 0 before the applied load reached about 100 kN, which indicated that substitute concrete with ECC can

significantly delay cracks in the beam. After that, the strain values along the stirrups increased quickly with the applied load. It can be found that the stirrup strain values of the ECC beam were much lower than those of the concrete beam for the same load value. For instance, the average stirrup strain for BRE20 is 2.34 times that of BRC20 at a load level of 180 kN. Once cracks occur in the concrete beam, concrete can provide very limited shear resistance. However, for the ECC beam, multiple tiny cracking of ECC material has little effect on its shear strength. Therefore, substitution of concrete with ECC material in a flexural member can significantly improve its shear load capacity and deformation ability.

3.3 Ductility evaluation

For concrete structures or members, the ductility coefficient μ is a very important parameter for defining the deformability at the ultimate load. For FRP materials, the stress-strain relationship is essentially linear and they rupture without any warning at ultimate loads. Hence, FRPs are always defined as high performance material with low ductility. Normally, the ductility coefficient μ is defined as the ratio of ultimate displacement to displacement at yielding point. Since FRPs have no yielding behavior and this definition is not suitable for FRP or FRP reinforced composites.

For FRP reinforced concrete member, two main approaches have been put forward to evaluating the ductility property. The first one is a deformation-based method, which was firstly proposed by Jaeger et al. to evaluate the

Table 3: Summary of ductility index by energy-based method

Series	Specimen ID	Total energy, N m	Elastic energy, N m	Inelastic energy, N m	Energy dissipation ratio, %	Failure mode
I	BRE12	6879.4	2008.8	4870.6	70.8	Flexural-tension
	BRE20	14495.2	3141.6	11353.6	78.3	Flexural-compression
	BRC20	7196.2	2877.4	4318.8	60.0	Flexural-compression
	BRE20-ns	4535.6	1240.0	3295.6	72.7	Shear-tension
II	BREC-C	8526.4	2266.4	6260.0	73.4	Shear-tension
	BREC-T	10581.3	2838.2	7743.1	73.2	Flexural-compression

ductility of FRP reinforced concrete members [16]. This ductility index takes considerations of the effect of strength or moment as well as the effect of displacement or curvature. The strength and deflection factors are defined as the ratio of load or deflection values at the ultimate state to the corresponding values at concrete compressive strain of 0.001. The compressive strain value of concrete (0.001) is often regarded as the beginning of inelastic energy dissipation. The compressive property of ECC is different from that of concrete not only in modulus of elasticity but also ultimate compressive strain capacity. So this ductility index based on deformation may not be appropriate for evaluating FRP reinforced ECC members. Another method for evaluating ductility property is energy-based approach, which was proposed by Naaman and Jeong in 1995 [7]. For this approach, the ductility index is expressed as the ratio of inelastic energy to the total energy of elastic and inelastic. The elastic energy can be calculated according to the unloading process of the member, or can be obtained from the area of the triangle determined by the average slope of the two initial stiffness of the load-deflection curve, as illustrated in Fig. 10. The failure point herein is defined as the point where the applied load drops to 80% of its peak load. Hence, in this paper, the ductility index based on energy dissipation is used for evaluating the ductility of the beam specimens.

Table 3 shows the summary of ductility indexes of all specimens. For specimens BRE12 and BRE20-ns, the elastic energy is estimated by the method illustrated in Fig. 10. For the other beams, the elastic energy is

directly calculated from the load-deflection curves. According to Table 3, it can be found that the energy dissipation ratios for FRP reinforced ECC beams are generally higher than that of FRP reinforced concrete beam no matter what failure mode happens. For beam BRE20, the elastic energy is very close to that of beam BRC20, while its total fracture energy and energy dissipation ratio are 100% and 30% larger than those of beam BRC20 respectively. Substitution of conventional concrete with ECC can significantly improve the inelastic energy dissipation ability. The energy dissipation of FRP reinforced beams is relevant to cracking mechanism of the matrix and interaction behavior between reinforcement and matrix. For FRP reinforced concrete beams, a large proportion of external work is stored as elastic energy in FRP and steel reinforcement and concrete, and the other part of external work is consumed to form cracks and inelastic deformation in concrete along the span. The stored elastic energy will recover during unloading process of the beam. That is why energy dissipation ratio is relative small for the FRP reinforced concrete beam. However, for FRP reinforced ECC beams, small amount of external work is stored as elastic energy in the reinforcement and ECC, and most of external work will be consumed to form multiple tiny cracks in the ECC material. Hence, for ECC beams, the inelastic energy takes a large proportion of the total energy. That is why the elastic energy of these two beams is similar while the inelastic energy dissipation is quite different.

The composite beams BREC-C and BREC-T show much higher ductility than that of the

concrete beam BRC20, which can be demonstrated by the total fracture energy and the energy dissipation ratio given in Table 3. For the ECC/concrete composite beam, the ductility is mostly related to the position and thickness of ECC layer. Based on current test results, the beam with ECC layer of 90 mm in the tension zone manifests better energy dissipation capacity than that of the beam with ECC layer in the compression zone. The total energy and inelastic energy dissipation of BRE-C-T are both about 1.24 times those of BRE-C.

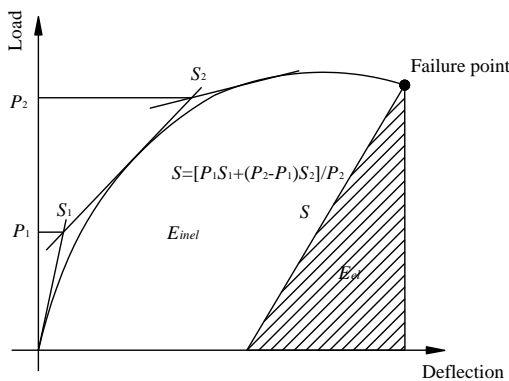


Fig 10 : The ductility index definition based on energy

4 CONCLUSION

In this paper, a number of FRP reinforced beams with different reinforcement configurations and matrix types have been tested under static loading conditions. For a FRP reinforced concrete beam, substitution of conventional concrete with ECC can significantly improve the flexural characteristics in terms of flexural strength, deformation capacity and energy dissipation ability. Based on the test results, the deformation capacity of the FRP reinforced ECC beam with reduced reinforcement ratio can show high deformation capacity due to high ultimate compressive strain of ECC materials. With the same geometric dimensions and FRP reinforcement configurations, ECC beam without stirrups showed comparable flexural strength and deformation performance with concrete beam with dense stirrups, indicating that the use of ECC can effectively enhance the shear capacity. The FRP reinforced ECC/concrete

beams can exhibit superior flexural performance to FRP reinforced concrete beam in energy dissipation ability. The composite beams with the ECC layer in the tension zone can show better deformation capacity than the beam with the ECC layer in the compression zone. Moreover, the ECC layer in the tension zone can avoid rupture failure of the FRP reinforcement in the ultimate stage. This may be attributed to many factors, such as the sensitivity of BFRP reinforcement to transverse stress concentration, the fiber bridging of ECC in the tension zone of the beam, and the compatible deformation between FRP reinforcement and ECC. In a word, the application of ECC in FRP reinforced beam member is quite effective in enhancing its flexural strength and deformation capacity, shear resistance, ductility and damage tolerance, compared with the proper designed FRP reinforced concrete beam member.

ACKNOWLEDGEMENT

Financial support of the work by National Natural Science Foundation of China under 51278118, by the National Basic Research Program of China (973 Program) under 2009CB623200 and the Priority Academic Program Development of Jiangsu Higher Education Institutions, is gratefully acknowledged.

REFERENCES

- [1] Vijay, P.V. and GangaRao, H.V.S., 2001. Bending behavior and deformability of glass fiber-reinforced polymer reinforced concrete members. *ACI. Struct. J.* **98(6)**:834-842.
- [2] Naaman, A.E., 2003. FRP reinforcements in structural concrete: assessment, progress and prospects. *Proc. of the 6th Int. Conf. on FRP. Reinforcement. for concr. struct.* 2003, Singapore: World Scientific; pp.1-24.
- [3] Sonobe, Y., Fukuyama, H., Okamoto, T., et al, 1997. Design guidelines of FRP

- reinforced concrete building structures. *J. Compos. Struct.* **1(3)**:90-113.
- [4] Theriault, M. and Benmokrane, B., 1998. Effect of FRP reinforcement ratio and concrete strength on flexural behavior of concrete beams. *J. Compos. Struct.* **2(1)**:7-15.
- [5] Naani, A., 1993. Flexural behavior and design of RC members using FRP reinforcement. *J. Struct. Eng.* **119(11)**:3344-3359.
- [6] Harris, H.G., Somboonsong, W. and Ko, F.K., 1998. New ductile hybrid FRP reinforcing bar for concrete structures. *ASCE. J. Compo. Constr.* **2(1)**:28-37.
- [7] Naaman, A.E. and Jeong, S.M., 1995. Structural ductility of concrete beams prestressed with FRP tendons. In L. Taerwe (eds), *Prco. of 2nd Int. RILEM (FRPRXS-2), Non-Metallic. (FRP) Reinforcement. of Concr. Struct*, 1995, London, Britain; pp.379-386.
- [8] Zhou, Y.W., Wu, Y.F., Teng, J.G., et al, 2009. Ductility analysis of compression-yielding FRP-reinforced composite beams. *Cem. Concr. Compo.* **31(9)**:682-691.
- [9] Kim, Y.Y., Fischer, G. and Li, V.C., 2004. Performance of bridge deck link slabs designed with ductile ECC. *ACI. Struct. J.* **101(6)**:792-801.
- [10] Lepech, M.D. and Li, V.C., 2009. Application of ECC for bridge deck link slabs. *RILEM. J. Mater. Struct.* **42(9)**:1185-1195.
- [11] Lepech, M.D. and Li, V.C., 2010. Sustainable pavement overlays using engineered cementitious composites. *J. Pavement. Res. Technol.* **3(5)**:241-250.
- [12] Zhang, J., Leung, C.K.Y. and Gao, Y., 2009. Simulation of crack propagation of fiber reinforced cementitious composite under direct tension. *Eng. Fract. Mech.* **78(12)**:2439-2454.
- [13] Fischer, G. and Li, V.C., 2002. Influence of matrix ductility on tension-stiffening behavior of steel reinforced engineered cementitious composites. *ACI. Struct. J.* **99(1)**:104-111.
- [14] Fisher, G. and Li, V.C., 2002. Effect of matrix ductility on deformation behavior of steel reinforced ECC flexural members under reversed cyclic loading condition. *ACI. Struct. J.* **99(6)**:781-790.
- [15] Maalej, M. and Li, V.C., 1995. Introduction of strain-hardening engineered cementitious composites in design of reinforced concrete flexural members for improved durability. *ACI. Struct. J.* **92(2)**:167-176.
- [16] Jaejer, L.G., Mufti, A.A. and Tadros, G., 1997. The concept of the overall performance factor in rectangular-section reinforced concrete beams. *Proc. of 3rd Int. Symp. on non-metallic. (FRP) reinforcement. Concr. Struct*, 1997, Sapporo, Japan; pp.551-558.